Astron. Astrophys. 345, L39–L42 (1999)

ASTRONOMY AND ASTROPHYSICS

LETTER

Letter to the Editor

IRAS 04296+3429: a 21 μm source with a very strong 30 μm emission band*

R. Szczerba[1,2], **Th. Henning**[3], **K. Volk**[2], **S. Kwok**[2], **and P. Cox**[4]

[1] N. Copernicus Astronomical Center, Rabiańska 8, PL-87-100 Toruń, Poland (szczerba@ncac.torun.pl)
[2] Department of Physics and Astronomy, University of Calgary, Calgary, Canada (Volk, Kwok@iras.ucalgary.ca)
[3] Astrophysikalisches Institut und Universitäts–Sternwarte, Jena, Germany, (henning@astro.uni–jena.de)
[4] Institut d'Astrophysique Spatiale, Université de Paris XI, Orsay, France (cox@ias.fr)

Received 15 January 1999 / Accepted 17 April 1999

Abstract. We report the detection of the 30 μm emission feature from the C-rich post–Asymptotic Giant Branch (post–AGB) star IRAS 04296+3429 based on ISO SWS observations. ISO data show that there is a clear substructure in the 30 μm feature in the form of a plateau which extends from 26 to 27 μm. This is confirmed by the ISO SWS data for another post-AGB object IRAS 22272+5435, which has the strongest known 30 μm band accounting for about 24% of its total infrared (IR) emission or 12% of the bolometric luminosity. In the case of IRAS 04296+3429 we estimate that about 85% of the total energy is emitted in the infrared of which about 15–22% (depending on the estimated continuum level) is contributed by the 30 μm band. The total energy emitted in the band is at least comparable for both sources, while the energy emitted in the 21 μm band seems to be about 3 times larger in the case of IRAS 04296+3429, if they have the same bolometric luminosity. Grains of pure MgS could be responsible for the observed 30 μm feature provided they have a broad distribution of shapes, but they cannot account for the observed plateau emission. Small graphite grains with relatively thick MgS coating could be responsible for the observed substructure, but we were not able to definitively solve the question of their contribution to the 30 μm band.

Key words: stars: AGB and post-AGB – stars: circumstellar matter – stars: individual: IRAS 04296+3429 – stars: individual: IRAS 22272+5435 – radiative transfer

1. Introduction

The 30 μm emission was first observed in the bright AGB star IRC+10216 (Low et al. 1973). Observations of several carbon stars by Goebel & Moseley (1985) found AFGL 3068 also to have this emission band. Recently, Infrared Space Observatory (ISO – Kessler et al. 1996) observations (see Yamamura et al. 1998 and Jiang et al. 1999) discovered this feature in some other C–rich AGB stars. This emission is also seen in C-rich post–AGB stars (see Omont et al. 1995) and planetary nebulae (see Forrest et al. 1981). A few suggestions for the carrier of this emission are proposed. Omont et al. (1995) suggested iron atoms bond to polycyclic aromatic hydrocarbon (PAH) molecules, while Goebel & Moseley (1985) first suggested solid magnesium sulfide (MgS) as a possible emitter for the 30 μm feature.

IRAS 04296+3429 (hereafter IRAS 04296) belongs to the small group of sources which show a spectral feature around 21 μm. As of early 1999, this feature has only been seen in C–rich post–AGB sources (see Kwok et al. 1999 for the most recent review) and for all of them which were observed by the Kuiper Airborne Observatory (KAO) the 30 μm feature is also detected (Omont et al. 1995). IRAS 04296 has not been observed by the KAO but detailed analysis of its spectral energy distribution (SED) allowed us (see Klochkova et al. 1998, 1999) to suggest that this source should also have the 30 μm feature. Our ISO observations have confirmed this supposition. In this paper we present the analysis of ISO SWS (de Graauw et al. 1996) spectra for IRAS 04296 and IRAS 22272+5435 (hereafter IRAS 22272), which show not only the 30 μm feature, but also clear evidence for its substructure.

2. ISO observations and data analysis

Spectra in the range from 23 to 43 μm for IRAS 04296 and IRAS 22272 were taken in 1997 (November and June, respectively) using ISO SWS 06 as part of the open time proposal RSZCZERB.PPN_30 to investigate the 30 μm feature in post–AGB objects. The original data were reprocessed using the Interactive Analysis software available at the MPE Garching[1], in

Send offprint requests to: Ryszard Szczerba (szczerba@ncac.torun.pl)

* Based on observations with ISO, an ESA project with instruments funded by ESA Member States (especially the PI countries: France, Germany, the Netherlands and the United Kingdom) and with participation of ISAS and NASA

[1] We acknowledge support from the ISO Spectrometer Data Centre at MPE Garching, funded by DARA under grant 50 QI 9402 3.

July, 1998. Final spectra have been obtained by using ISO Spectral Analysis Package v1.5. Details of the analysis are given below.

2.1. IRAS 22272+5435

The SWS 06 spectrum for IRAS 22272 is of very good quality. However, there is a significant jump (about 18%) between bands 3E (27.5–29.0 μm) and 4 (29–43 μm) in direction opposite to what would be inferred from the difference in area of the sky seen in these two bands. Our SWS 06 spectrum includes two additional small scans (28.7–29.5 μm) covering the region between bands 3E and 4. They agree with the continuum level of band 3E but do not with that of band 4 (shown as a dashed line in Fig. 1). After scaling the band 4 data by a factor of 1.18, they agree with the data of band 3E and the resultant spectrum is plotted as a solid line between 23 and 43 μm.

For IRAS 22272, the KAO data (Omont et al. 1995) are also plotted in Fig. 1 (open circles). We can see that the KAO data agree well with the ISO SWS 06 bands 3E and 3D (here 23.0–27.5 μm), except that the 26–27 μm plateau seen in the ISO data is not clearly resolved by the KAO. Note, however, that there is some problem with band 3D data for wavelengths longer than about 26 μm from leakage from shorter wavelengths and from an extrapolation of the relative spectral responsivity function. These two effects act in opposite manners and tend to cancel each other out, thus the error for the low colour temperature post-AGB objects is expected to be small (no more then a few percent: S. Hony, private communication). The lack of agreement between the KAO and band 4 data can be related to the KAO and/or ISO band 4 calibration (the same problem is seen in the spectrum of IRAS 07134+1005, Hrivnak et al. 1999).

2.2. IRAS 04296+3429

There were serious difficulties in reducing the SWS 06 band 4 data for this object. Most of the detectors were badly affected by cosmic ray glitches, so that the automatically processed band 4 spectrum was almost totally useless. However, we are encouraged by the fact that there are no significant jumps between SWS bands 3D, 3E and 4. After carefully examining the scans for each of the 12 detectors in both the "up" and "down" directions we decided to use the data for the four detectors only (40, 42, 47 and 48): the other eight detectors had much worse dark current levels and were much more prone to glitches.

Using only these four detectors we carried out data manipulation in the ISAP software to remove some remaining glitches and average the values (we choose a wavelength interval of 0.15 μm for the averaging). The ISAP averaging procedure resulted in a reasonably smooth spectrum which is generally consistent between the "up" and "down" scans. The point to point fluctuations are of the order of 1 to 2 Jy, or about 2 to 4% of the continuum level at the short wavelength end of band 4. From comparison of the "up" and "down" scans along with the point to point fluctuations we estimate that the actual uncertainty in the points in band 4 is at about the 2 to 3 Jy level, or about 5 to 10% depending upon which part of the spectrum is considered. The overall spectral shape appears to be trustworthy, but the small scale structures on the continuum are not reproducable between the "up" and "down" scans and therefore cannot be trusted (e.g. bump between 33–36 μm is rather related to the strong glitches in this wavelength region).

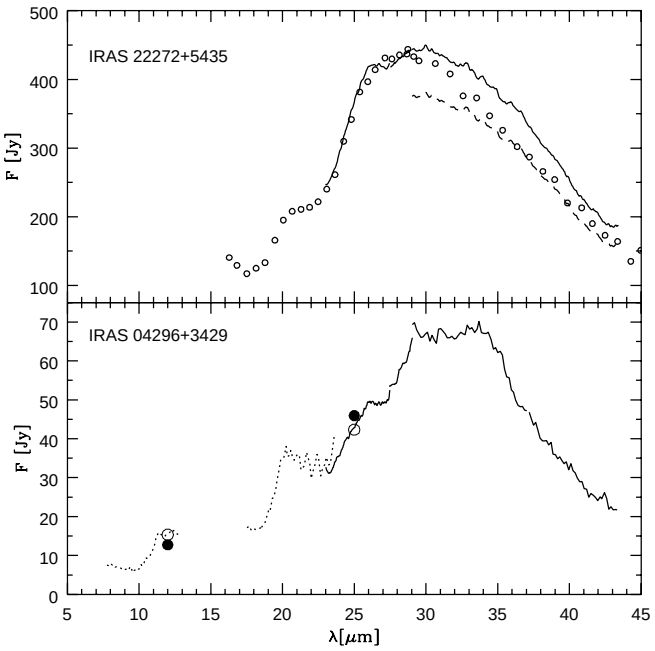

Fig. 1. ISO SWS 06 spectra for two 21 μm sources. *Top:* The ISO SWS 06 spectrum for IRAS 22272 is shown as a solid line in the range from 23 to 43 μm. The open circles are KAO observations. The dashed line shows the band 4 spectrum before scaling (see text). *Bottom:* The same as above but for IRAS 04296. In addition, the CGS3 spectra are shown as dotted lines and the IRAS 12 and 25 μm PSC fluxes are coded as filled circles before and as open ones after color–correction.

The resultant SWS 06 spectrum is shown as a solid line in Fig. 1. We can see that there is a reasonably good agreement between bands 3D and 3E (at 27.5 μm) as well as between 3E and 4 (at 29 μm). Again, as it has been mentioned above, there could be a small problem with data for $\lambda > 26\,\mu$m which, however, seems to be not crucial. Also plotted in Fig. 1 are the UKIRT CGS3 spectra (shown as dotted lines from 7.7 to 12.9 μm and from 17.5 to 23.6 μm), kindly provided by K. Justtanont (Justtanont et al. 1996). Interpolation of flux between two CGS3 bands and integration with the IRAS 12 μm band response function gives 9.2 Jy, which is about 38% lower than the PSC flux at 12 μm (12.7 Jy). Although the IRAS LRS spectrum is available for IRAS 04296 (e.g. University of Calgary IRAS Data Analysis Facility), it is of lower signal-to-noise than the CGS3 spectra. In fact, an convolution of the LRS spectrum with the IRAS 12 μm profile gives 9.4 Jy (value similar to that one obtained for the CGS3 spectra). On the other hand, convolution of the CGS3 and SWS 06 data with the IRAS 25 μm band profile yields a flux of 38.0 Jy, which is about 20% lower than the PSC flux at 25 μm (45.9 Jy), while similar integration for the LRS spectrum

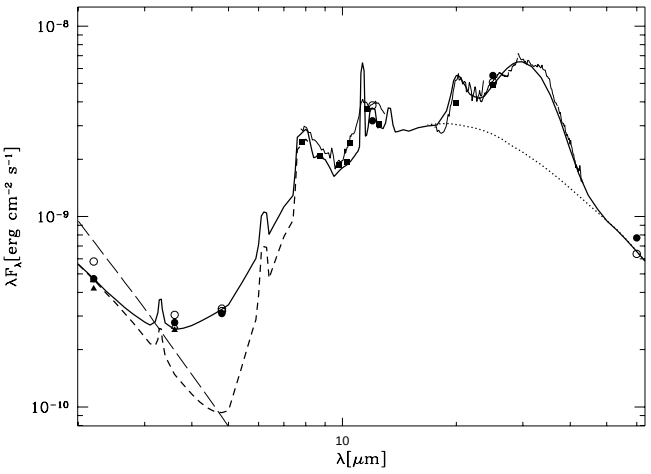

Fig. 2. Model fit of the SED for IRAS 04296+3429 taking into account quantum heating effects (solid line) and assuming that the star radiates according to a model stellar atmosphere calculation for log(g) = 0.5 and T_{eff} = 6500 K (long–dashed line). The short–dashed line shows fit obtained when hot dust was removed. The dotted line for wavelengths $> 18\,\mu$m represents the continuum level. Observational data are described inside the text.

roughly agrees with the PSC flux. Note, that the SWS 06 spectrum around 21 μm (Volk et al. 1999) has a flux density level about 50% lower than the LRS one.

3. Modelling of the spectral energy distribution

The SED of IRAS 04296 has previously been fitted (see Klochkova et al. 1998, 1999) for a mixture of PAH and amorphous carbon (AC - Rouleau & Martin 1991) grains with an empirical opacity function (EOF) added to reproduce the 21 and 30 μm features. Such approach allowed us to take approximately into account absorption of the visual radiation by the carrier(s) of these features. The grains are assumed to have a size distribution from 5 to 10 Å for PAH, and of 50 Å to 0.25 μm for AC (see Szczerba et al. 1997 for more details). Here, we have repeated the computations taking into account the new ISO results.

It has been shown on the basis of the ISO SWS 06 observations that the normalized shape of the 21 μm feature is the same for all the observed sources (Kwok et al. 1999, Volk et al. 1999). Therefore, the normalized profile of IRAS 07134+1005 (the strongest 21 μm emitter) is assumed as EOF for the 21 μm feature, whereas the 30 μm feature is approximated by the sum of two half–gaussians with the same central wavelength (30 μm) but with different widths. The width at half maximum is assumed to be 6.0 μm for the short–wavelength side and 8.0 μm for the long–wavelength side. Note that the assumed gaussian profile has no physical meaning and is only used for a convenient representation of the 30 μm band. A superposition of the EOF's for the 21 and 30 μm features (with strength found during the model fitting procedure) was added onto the mass absorption coefficient of AC grains with radius of 0.1 μm.

In Fig. 2 we show part of the fit to the SED of IRAS 04296 (fit for the shorter wavelengths is very similar to that presented in Klochkova et al. 1999), together with additional data: photometry from Hrivnak and Kwok (1991) in near–infrared (NIR) bands (filled circles); their photometry in mid–infrared (MIR) bands (filled squares); and NIR photometry from Manchado et al. 1989 (filled triangles). We present also two sets of photometry (from K to M band) corrected for interstellar extinction according to the average extinction law of Cardelli et al. (1989) for A_V of 1.0 or 2.0 magnitudes (see Klochkova et al. 1999).

The best fit obtained assuming the EOF described above (see Table 2 in Klochkova et al. 1999 for details concerning adopted parameters) is shown by the solid line. Since the adopted EOF is different from that used before and, in addition, since we try to model the original CGS3 data (i.e. without normalization to the IRAS PSC fluxes), it was necessary to tune up parameters to obtain a fit which can account for all of the presented data. This was done by increasing the distance of the source from 5.4 to 5.6 kpc, making the main shell slightly cooler (dynamical age has been increased from 575 to 625 yrs), changing density distribution inside the main shell (from $\sim r^{-2.6}$ to $\sim r^{-2.3}$) and introducing necessary changes (about 20%) in mass loss rates during AGB and post–AGB phases of evolution. The total dust mass is about 0.01 $M_\odot$.

The dotted line for $\lambda > 18\,\mu$m represents the estimated continuum level for dust without EOF but with the same parameters (including dust temperatures) as for the case of dust with EOF. Taking into account this continuum level, we estimate the energy emitted in the 21 μm band to be about 5% of the total IR flux and in the 30 μm band to be about 22% of the total IR emission (compare to about 24% in the case of IRAS 22272). However, in the case of IRAS 04296 the total IR flux is about 85% of the total energy emitted by the source, while in the former case it is only about 50%. In consequence, if the luminosities of these two sources were the same, then the amount of energy emitted in the 30 μm band would be larger in the case of IRAS 04296. On the other hand, a fit to the normalized CGS3 data (i.e. to data which agree with the IRAS PSC fluxes) gives a higher continnum level and a smaller energy in the 30 μm band (about 15% of the total IR luminosity) which translates to a similar total energy emitted in this band for both sources, if they have the same bolometric luminosity.

4. Discussion

We have taken up the suggestion by Goebel & Moseley (1985) and tested the possibility that MgS (optical data for this material have been taken from Begemann et al. 1996) could be responsible for the 30 μm feature. The method described in Szczerba et al. (1997) was used to estimate how much sulphur bonded in MgS would be required to explain the observed strength of the 30 μm emission. In Fig. 3 we present a comparison between the 30 μm feature after the continuum subtraction (see Fig. 2) and emission from MgS grains. The presented results have been estimated assuming that $2.0\,10^{-6}$ of n(S)/n(H) is bonded in each form of MgS grains. The largest contribution comes from the

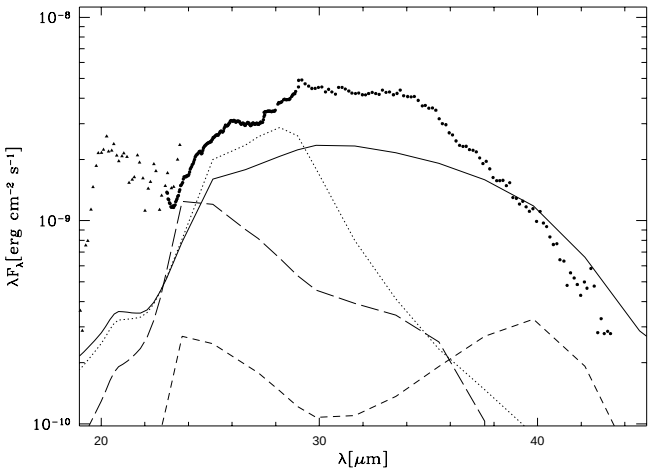

Fig. 3. Comparison between the 30 μm feature after continuum subtraction (filled circles) and emissions from different forms of MgS grains: ellipsoidal (solid) and spherical (dotted line). Short-dashed and long–dashed lines present contribution from the small AC and small graphite grains coated with MgS, respectively. The triangles show part of the CGS3 spectrum also after the continuum subtraction.

ellipsoidal (continuous distribution of ellipsoids - CDE) grains (solid line) and the spherical ones (dotted line). In principle, grains of pure magnesium sulfides could be responsible for the observed 30 μm emission provided they have an appropriate broad distribution of shapes. The total amount of n(S)/n(H) required is smaller than the total sulphur abundance found in the photospheric spectrum (n(S)/n(H) = $6.3\,10^{-6}$ with a possible range between 3.9 and $10\,10^{-6}$, Klochkova et al. 1999), so the sulphur abundance does not seem to pose a problem for the MgS model. However, the pure MgS contribution cannot explain the observed plateau emission between 26 and 27 μm. Therefore, we have "experimented" with AC and graphite grains (Laor & Draine 1993) coated with MgS. Since mass absorption coefficients of such grains depend strongly on the relative thickness of the mantles, small grains are required to satisfy the sulphur abundance constraints. This is because core grains with larger radius need more coating material to have the same relative thickness of the coats. The method used to compute mass absorption coefficients and discussion of the MgS coats on AC grains is described in Szczerba et al. 1997 (see also their Fig. 3). Here, we assume that AC grains with radii smaller than 100 Å are coated by the MgS in amount determined by n(S)/n(H) = $2.0\,10^{-6}$. This results in relative thickness of the MgS coats ranging from about 4.5% for 50 Å up to 2.3% for 100 Å grains. Emission from such grains is shown as a short–dashed line in Fig. 3. It is clear that AC grains coated with MgS are the less efficient absorbers and do not contribute to the observed maximum at around 26 μm.

We have also checked the possibility of contribution from small graphite grains coated with MgS. The same amount of sulphur in the mantle and the same amount of mass (relative to the gas) of graphite grains ($5\,10^{-4}$) are assumed as in the previous case. However, the sizes of graphite cores vary now from 5 Å (relative thickness 11%) to 50 Å (relative thickness 1.3%). The results are shown as a long–dashed line in Fig. 3. There is a plateau in their emission similar in shape to the observed one, but shifted by about 2 μm to the shorter wavelengths. It could rule out the possibility of contribution by small graphite grains coated with MgS, but note, that with relatively thicker MgS coats (which would require however more S bonded into coats) the maximum will shift to about 25 μm. It is still about 1 μm less than the observed one, but it could be that core grains of different than spherical shape will create the maximum at the required wavelength.

Finally, let us discuss shortly possible correlation between 21 and 30 μm features. As it has been mentioned in the Introduction all 21 μm emitters which have been observed up to now around 30 μm have shown this feature. In addition, on the basis of the available pre–ISO data we were able to show that the other 21 μm source IRAS 05113+1347 (Szczerba et al. 1996) as well as IRAS 05341+0852 and IRAS 22223+4327 (see in Kwok et al. 1995) should have the 30 μm band as well. This could mean that these two features share a common origin, or are at least related to each other. This suggestion is supported by other ISO SWS 06 spectra (Szczerba et al., in preparation) which show that all 21 μm sources observed by us seem to have the 30 μm band as well.

Acknowledgements. We are very grateful to the referee Iseei Yamamura for the critical reading of the manuscript. This work is in part supported by the grant 2.P03D.002.13 to RS from the Polish State Committee for Scientific Research and by CNRS: "jumelage France–Pologne" and in part by a grant to SK from the Natural Sciences and Engineering Council of Canada.

References

Begemann B., Dorschner J., Henning Th. et al. 1994, ApJ 423, L71
Cardelli J.A., Clayton G.C. & Mathis J.S. 1989, ApJ 345, 245
Forrest W.J., Houck J.R. & McCarthy J.F. 1981, ApJ 248, 195
Goebel J. & Moseley S. 1985, ApJ 290, L35
de Graauw T., Haser L., Beintema D. et al. 1996, A&A 315, L38
Hrivnak B.J. & Kwok S. 1991, ApJ 368, 564
Hrivnak B.J., Kwok S., & Volk K. 1999, in preparation
Jiang B.W., Szczerba R., & Deguchi S. 1999, A&A 344, 918
Justtanont K., Barlow M.J., Skinner C.J. et al., 1996, A&A 309, 612
Kessler M.F., Steinz J.A., Anderegg M.E. et al. 1996, A&A 315, L27
Klochkova V.G., Panchuk V.E. & Szczerba R., 1998, Ap&SS 255, 485
Klochkova V.G., Szczerba R., Panchuk V.E. & Volk K. 1999, A&A (in press)
Kwok S., Hrivnak B.J. & Gebale T.R. 1995, ApJ 454, 394
Kwok S., Volk K. & Hrivnak B.J. 1999, in *IAU Symp. No. 191: Asymptotic Giant Branch Stars*, eds. T. Le Bertre, A. Lébre, and C. Waelkens, ASP Conf. Ser., p. 297
Laor A., Draine B.T. 1993, ApJ 402, 441
Low F., Rieke G. & Armstrong K. 1973, ApJ 183, L105
Manchado A., Pottasch S.R., Garcia-Lario P. et al. 1989, A&A 214, 139
Omont A., Moseley S., Cox P. et al. 1995, ApJ 454, 819
Rouleau F., Martin P.G. 1991, ApJ 377, 526
Szczerba R., Volk K. & Kwok S. 1996, in *The role of dust in formation of stars*, ESO Workshop, eds. Käufl H.U., Siebenmorgen R., p.95
Szczerba R., Omont A., Volk K. et al. 1997, A&A 317, 859
Volk K., Kwok S. & Hrivnak B.J. 1999, ApJ (in press)
Yamamura I., de Jong T., Justtanont K. et al. 1998, Ap&SS 255, 351